Spin-echo envelope modulation study of $LaF_3:Nd^{3+}$

D. W. Hess* and L. G. Rowan
Department of Physics and Astronomy, University of North Carolina, Chapel Hill, North Carolina 27514
(Received 18 April 1978)

A pulsed-electron-spin-resonance experiment has been performed on a single crystal of lanthanum trifluoride containing 0.1 molar per cent of neodymium impurity. The purpose of the experiment was to measure the superhyperfine coupling between the magnetic moments of the ligand fluorine nuclei and the magnetic moment of the $4f$ electronic spin belonging to the neodymium ion. The experiment employed the technique of spin-echo envelope modulation. Modulation envelopes were obtained at five orientations of the laboratory magnetic field. The interaction parameters were determined by comparing the experimentally derived modulation envelopes with the computed theoretical modulation curves. Under the assumption that all of the near nuclei interact with equal strengths, it was found that the isotropic interaction parameter $A = -1.5 \pm 0.5$ MHz and that the dipole-dipole or anisotropic parameter $D = 4 \pm 1$ MHz. The negative value of A implies that the $4f$ electronic spin in the vicinity of the ligands is parallel to the net spin of the neodymium ion. The value of D that was measured is greater than what would be expected if the interaction were purely of the classical point-dipole type. Therefore, some covalent bonding involving neodymium f orbitals and fluorine p orbitals must be present.

I. INTRODUCTION

The purpose of this work is to measure the electron-spin–ligand–nuclear interaction or superhyperfine (shf) in the physical system $LaF_3:Nd^{3+}$ using the technique of electron spin-echo envelope modulation. The fluorine ions which surround the Nd^{3+} ion possess nuclei which have magnetic moments associated with their spin angular momentum. The interaction between the $4f$-electron magnetic moment and the fluorine nuclear magnetic moment is the object of this study.

The technique of electron spin-echo envelope modulation was first employed by Rowan, Hahn, and Mims[1] to study the SHF interaction of $CaWO_4$: Ce^{3+} and has been observed in other systems as well.[2,3] Since it was first observed, interest in echo envelope modulation has been maintained[4-9] and the essential ideas carried over to photon echo experiments.[9,10]

The shf interaction has been studied using the electron-nuclear-double-resonance (ENDOR) technique.[11,12] ENDOR is presently the standard method of obtaining the shf parameters, in those cases where the inhomogeneous broadening is large. The electron spin-echo envelope modulation is an alternate way of measuring these same parameters.

Section II discusses the structure of LaF_3; Sec. III discusses the experimental and computational procedure; and Sec. IV discusses the results.

II. STRUCTURE OF $LaF_3:Nd^{3+}$

Lanthanum trifluoride is doped with neodymiun trifluoride to yield $LaF:Nd^{3+}$. The ion Nd^{3+} has a $4f^3$ ground-state configuration leading to a ground state term of $^4I_{9/2}$. Since the L-S coupling is not a good approximation in the rare earths, the ground state wave function is admixed with other terms giving[13]

$$|^4I_{9/2}\rangle = 0.984\,|^4I\rangle - 0.166\,|^2H\rangle.$$

The electrostatic crystal field at the ion site in LaF_3 is of rather low symmetry; characterized only by a single C_2 axis that is normal to the c axis of the crystal. This crystal field splits the $^4I_{9/2}$ levels into five twofold Kramers-degenerate levels.[14,15]

Upon application of an external magnetic field, the Kramers-degenerate levels are split. This Zeeman splitting can be expressed in terms of an effective spin and a g tensor. Thus we arrive at an effective Hamiltonian with a spin of $\frac{1}{2}$ and an anisotropic g tensor.

The space group of LaF_3 is still in question. The studies of the vibrational modes of LaF_3 together with the most recent x-ray diffraction experiment strongly support the assignment of D_{3d}^4 ($P\bar{3}c1$) as the proper space-group symmetry for the tysonite fluorides.[16-23] However, there is a discrepancy between the magnetic resonance data[24-28] and the x-ray and optical phonon data. The electron paramagnetic resonance (EPR) data shows six magnetically inequivalent ions per unit cell, the six sites being related by 120° rotations about the c axis and by reflections in a plane perpendicular to the c axis.

For the purposes of analyzing the results of this experiment, the structure of LaF_3 is assumed to

 ©1979 The American Physical Society

be D_{3d}^4. The geometrical relationship of the Nd^{3+} ion to its fluorine neighbors is taken to be that which is given by the x-ray diffraction results of Zalkin, Templeton, and Hopkins.[21] The experimental results reported here are in agreement with the hypothesis that there exists a mirror twin, or equivalently a rotation twin within every LaF_3 crystal and that the crystal is composed of equal amounts of each twin. Presumably the crystal is twinned on a microscopic scale in a balanced fashion. In view of the very low activation energy for the formation of Schottky defects (0.07 eV) and the low activation energy for fluorine diffusion (0.45 eV), it seems very likely that the crystal might be twinned because the existence of vacancies would allow microscopic twins to coexist easily.

A. Orientation of the sample

Baker and Rubins[24] found that the g tensor for this system is characterized by principal values $g_x = 1.356$, $g_y = 1.092$, $g_z = 3.11$; they describe the axis system in which the g tensor is diagonal as one whose y axis is perpendicular to the crystal c axis and whose z axis is tilted away from the c axis by an angle of $45° \pm 2°$. Furthermore they report that there are six equivalent g tensors which are derived from one another by rotations about the crystal c axis by 120° and 240° and by reflection in the plane perpendicular to the c axis. This data has been verified by Schulz and Jeffries[25] and by Wong, Staffsudd, and Johnston.[26] Schulz and Jeffries determined that the y axis of the g tensor is perpendicular to one of the cleavage planes; although they were using the most recent x-ray data these authors do not state which plane of the D_{3d}^4 structure this cleavage plane is. Assuming that the structure D_{3d}^4 is correct, one can show by the simple argument which follows that the y axis of the g tensor must like in an a-c plane of the crystal. In the D_{3d}^4 structure, the metal ion site possesses C_2 symmetry and the twofold rotation axis is perpendicular to the c axis of the crystal. The g tensor of LaF_3:Nd^{3+} possesses only one axis that is perpendicular to the c axis of the crystal; by definition, this axis is the y axis of the g tensor. If there is a single symmetry axis for a particular cation site, the one of the axes of the g tensor must coincide with that symmetry axis. Hence it follows that the y axis of the g tensor must coincide with the C_2 axis of the cation site. Since the C_2-axis lies in an a-c plane, the y axis of the g tensor also lies in an a-c plane.

The orientation of the crystalline axes of the sample relative to the laboratory frame was determined in two ways. First, a series of four Laue x-ray photographs was made using different orientations of the cylindrically shaped sample in order to locate the c axis of the crystal. When the c axis was found, the sample was then placed in the waveguide of the spin-echo spectrometer in such a way that the c axis was approximately perpendicular to the plane of rotation of the constant magnetic field. This arrangement had the c axis nearly vertical and the laboratory field H_0 capable of being rotated in the horizontal plane in the conventional way. Then, secondly, a map of the resonance lines was made by recording and plotting the values of the field H_0 which produced echo signals. Once the field map had been obtained, the orientations of the g-tensor axes relative to the laboratory frame could be found by identifying the orientation which reproduced the map of the resonance lines theoretically. The results of the field mapping show six strong resonance lines for values of H_0 above about 4 kG. For values of H_0 below about 4 kG the spin-echo signal was very weak. It was possible, though tedious, to follow the lines through their low-field regions.

B. Nd^{3+} ion and its fluorine ligand nuclei

The analysis of the experimental data considers only the set of eleven nearby fluorine neighbors to be of importance in the ligand hyperfine interaction. The six sets of fluorine ligand groups fall into two categories of three sets each. The three members of the first category differ from one another by rotations of $\pm 120°$ about the c axis; similarly for the three members of the second category. The two categories are related by the inversion operation carried out through the origin of the coordinate system located at the metal ion site.

It can be shown that the g tensor for a given cation site is unchanged when the inversion operation is applied to the D_{3d}^4 structure. This is the basis for the discrepancy that exists between EPR data and the results of experiments showing that the structure is D_{3d}^4; EPR data show six magnetically inequivalent sites whereas the D_{3d}^4 structure has only three. It is assumed, therefore, that all the tysonite fluorides are twinned and this discussion proceeds on that assumption. It is supposed that within the sample there are regions which differ from one another by mirror reflection through the basal plane of the D_{3d}^4 structure, or equivalently by two-fold rotation about the c-axis.

III. SPIN-ECHO ENVELOPE MODULATION EXPERIMENT

The experiment consists of varying the time interval τ between two pulses of microwave radiation whose frequency corresponds to the Zeeman energy splitting of the Nd^{3+} Kramers ground state and then recording the amplitude of the echo signal

as a function of τ. In general there is always a loss of amplitude as the pulse spacing is increased due to relaxation; this is generally an exponential decay and is slowly varying when compared to the effects of the nuclear interaction on the echo signal. The total echo envelope is the curve resulting from a plot of the peak echo amplitude versus pulse spacing; it contains information on the spin-phonon interaction as well as the spin-nuclear interaction. The modulation envelope is the envelope after the exponential decay has been removed; it contains only spin-nuclear information.

A. Experimental data

The LaF_3 sample containing 0.1 mole% of Nd was obtained from Optovac, Inc. of North Brookfield, Mass. (i.e., one ion of Nd for each 1000 La ions). The cylindrical sample was sawed rather than cleaved; its dimensions were 10-mm diam by 4 mm thick. Laue photographs of the sample showed that the crystalline c axis made an angle of approximately 60° with the cylinder axis.

The sample was placed in an open wave guide (no cavity) of the spectrometer arm which extended downward into a glass dewar containing liquid helium at 4.2 °K. This arm of the spectrometer was filled with styrofoam to keep liquid helium out of the waveguide.

The pulses used for this experiment were 12 nsec in width and approximately 1 kW in peak power. The experiment was performed with both pulses of equal width in order to insure that a uniform bandwidth of spins was excited by both pulses. The frequency of the signal klystron was 9000 MHz as measured on the cavity wave meter.

The minimum pulse spacing for which echoes could be detected was approximately 250 nsec; the reason is that the transmitter traveling wave tube requires some time to cut off and to stop producing its background noise.

The echo signals were photographed with a Polaroid scope camera. The modulation data were taken with the scope trace starting at the peak of the second pulse, so that the horizontal axis of the scope graticule could be labelled as the pulse spacing τ. Multiple exposure photographs were taken of the echo as the pulse spacing was varied from 0 to 1μsec. The two-pulse sequence was repeated at a rate of 100/sec; a single multiple exposure photograph required several minutes of time to produce; so that a spin-echo modulation envelope was made up of about 10^4 echo pulses.

The echo signals for field values below 4 kG were extremely weak. However, the echo signals for field values above 4 kG were strong enough that they could be displayed on the oscilloscope following detection just after the receiver travelling wave tube. It was also true that the i.f. amplifier tended to widen the pulses from 12 nsec to approximately 30 nsec. The envelope modulation was found to be rapid enough and deep enough that there was a marked difference in the modulation depth of the multiple exposure photos for 12- and 30-nsec echo widths. Hence it was decided to concentrate on the regions of magnetic field where the signal was strong enough to make i.f. amplification unnecessary. As it turned out, the fit of the theoretical model to the experimental data was not sufficiently good to discriminate whether the twinning hypothesis is valid.

The data consisting of the five modulation envelopes were reduced from the oscilloscope multiple exposure photographs by projecting the polaroid photos onto a piece of 7-×10-in. graph paper ruled 10×10 lines per $\frac{1}{2}$ in. The magnification of the projector was adjusted in such a way that the projected image of the scope graticule (real size 4×10 cm) was 4×10 in. Each square centimeter of scope graticule thus contained a 20×20 line grid after the projection process. The modulation envelope was recorded on the graph paper by tracing the black-white border of the multiple exposure photograph.

The data were replotted on three-cycle semilogarithmic graph paper. A sloping straight line was then drawn along the peaks of the echo envelope to represent the exponential decay. The difference between the echo envelope and the straight line was then measured with a divider and transferred for convenience to the top of the logarithmic graph paper; so that the slope was removed from the echo envelope, leaving the experimental modulation curve as the reduced data.

The reduced experimental data are shown in Figs. 1–5 graphed in the lowest cycle of the semilogarithmic plot; the upper curves in Figs. 1–5 are the best fits to the data generated using the computer program.

B. Theoretical analysis

In order to analyze the experimental results, the theoretical version of the modulation curves are generated using a computer program written by Rowan. The modulation curves generated were then compared to the experimentally derived modulation curves for a variety of the model parameters; the judgment of best fit was done by eye rather than the least-squares measure because it was expected that the rapid oscillations of the function would give rise to numerous local minima making the least-squares parameter unreliable.

The form of the modulation function for ligand nuclei of spin $\frac{1}{2}$ is particularly simple; for the ith nucleus the modulation curve is given by[1]

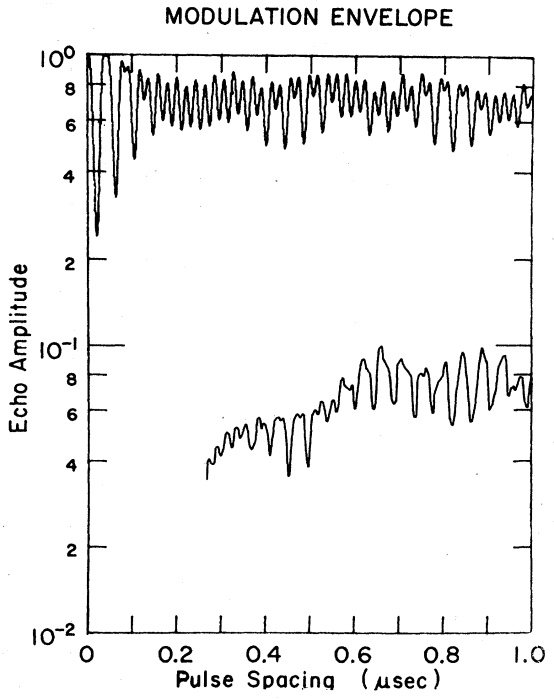

FIG. 1. Upper curve is the calculated echo envelope from the computer program for A_{lab} equal to 134° (see Table I). The applied field is along the y axis of the g tensor. The lower curve is the measured echo envelope with the relaxation decay removed. Echo amplitude is in arbitrary units and the pulse spacing is the time, in microseconds, between the two microwave pulses.

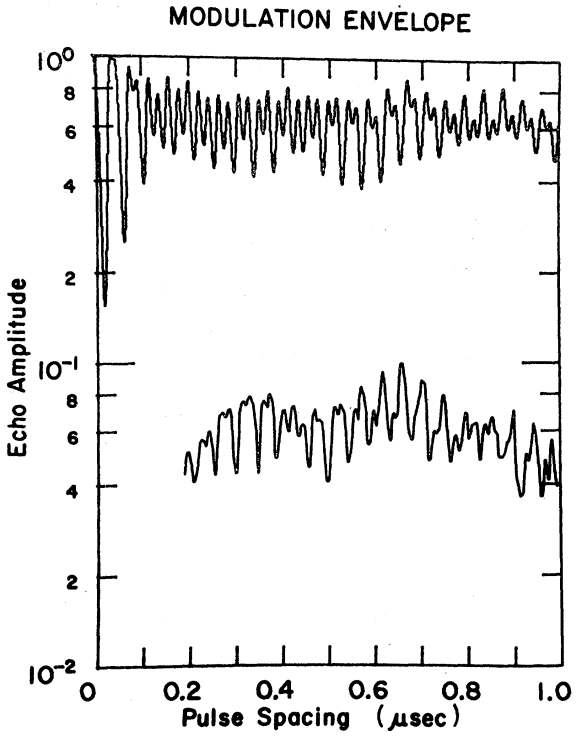

FIG. 2. Upper curve is the calculated echo envelope from the computer program for A_{1ab} equal to 129° (see Table I). The applied field is - 5° from the y axis of the g tensor in a plane approximately perpendicular to the c axis of the crystal. The lower curve is the measured echo envelope with the relaxation decay removed. Echo amplitude is in arbitrary units and the pulse spacing is the time, in microseconds, between the two microwave pulses.

$$v_i = \frac{V_i}{V_{0i}} = G_{1/2}(-\tfrac{1}{2}, \tau, \tau)$$

$$= 1 - 2\sin^2\delta_1(\sin\tfrac{1}{2}K_i^+\tau)^2(\sin\tfrac{1}{2}K_i^-\tau)^2,$$

$$\sin^2\delta_i = (2b_i\omega_i/K_i^+K_i^-),$$

$$K_i^\pm = [(\omega_{Ni} \pm \tfrac{1}{2}a_i)^2 + (\tfrac{1}{2}b_i)^2]^{1/2},$$

where ω_i is the nuclear Larmor frequency of the ith ligand nucleus. The quantities a_i and b_i can be calculated as in reference 1 with the parameters ϕ_r and θ_r having the subscript i added in order to specify the particular Ligand nucleus referred to. Alternatively, as is done in the program, the parameters $K_i^\pm$ is the nuclear splitting of the ith ligand when the electron spin is up (+) or down (−).

The modulation curve for the system of eleven ligand nuclei is then found from $V = \prod_{i=1}^{11} |v_i|$. The interaction Hamiltonian which describes the electron-spin-ligand-nuclear interaction can be written

$$H_{\text{int}} = \sum_{i=1}^{11} [D_i \vec{I}_i \cdot (3\hat{r}_i\hat{r}_i - \vec{1}) \cdot \vec{g} \cdot \vec{S} + A_i \vec{I}_i \cdot \vec{g} \cdot \vec{S}].$$

The parameters A_i and D_i portray the strength of the two kinds of interaction that are possible in the model for each of the ligand nuclei; these two parameters along with the direction cosines of H_0 and of the ith position vector $\hat{r}_i$ go into the makeup of a_i and b_i.

It should be kept in mind that other authors write H_{int} in a slightly different form and omit the g tensor from the two terms; instead a general superhyperfine tensor is used to characterize the entire Hamiltonian, which is then divided into an isotropic and an anisotropic term

$$H_{\text{int}} = \sum_i [A_s \vec{S} \cdot \vec{I} + A_p(3I_zS_z - \vec{I} \cdot \vec{S})].$$

Since much of the work on ligand ENDOR has been done on ions in CaF_2 where the g tensor has three

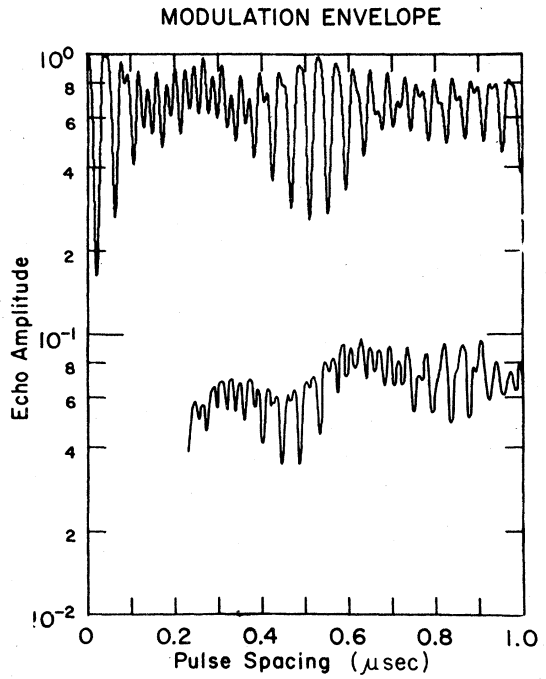

FIG. 3. Upper curve is the calculated echo envelope from the computer program for A_{1ab} equal to 139° (see Table I). The applied field is +5° from the y axis of the g tensor in a plane approximately perpendicular to the c axis of the crystal. The lower curve is the measured echo envelope with the relaxation decay removed. Echo amplitude is in arbitrary units and the pulse spacing is the time, in microseconds, between the two microwave pulses.

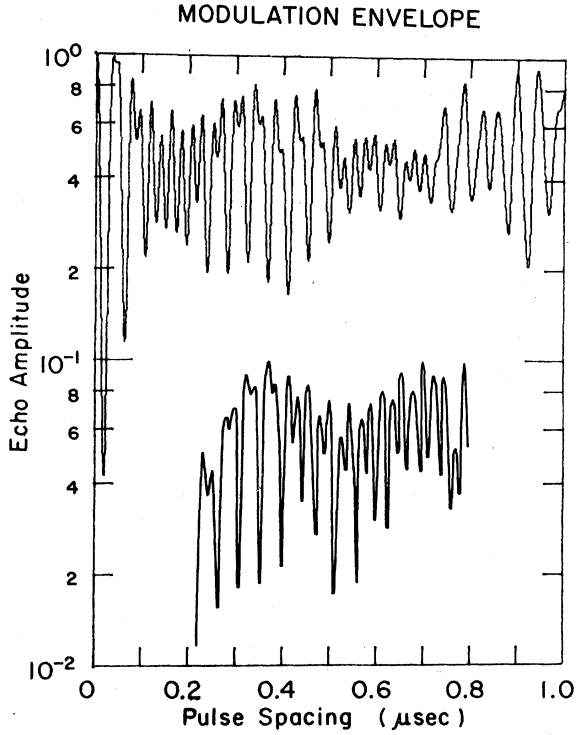

FIG. 4. Upper curve is the calculated echo envelope from the computer program for A_{1ab} equal to 124° (see Table I). The applied field is −10° from the y axis of the g tensor in a plane approximately perpendicular to the c axis of the crystal. The lower curve is the measured echo envelope with the relaxation decay removed. Echo amplitude is in arbitrary units and the pulse spacing is the time, in microseconds, between the two microwave pulses.

equal principle values, this is entirely satisfactory. For anisotropic g tensors the form which includes the g tensor is more appropriate from a physical point of view.[1,29,30,32]

IV. RESULTS

Figures 1–5 display the experimental data and the theoretical computer plots which were fit by adjusting the parameters of the model. Due to the limitations on computer time available, it was necessary to be content with fits of the theoretical model to the experimental data which are less than perfect and in fact not as good as what it is ultimately possible to achieve. The curves which are displayed were obtained by making the simplifying assumption that all of the ligand nuclei have the same strengths of dipole-dipole interaction and of isotropic interaction. That is, $A_i = A$, $i,j = 1,2,\ldots,11$, $D_j = D$. The goodness of fit was judged by eye and an effort was made to find that value of A and that value of D which yielded the best matches between theory and experiment for all of the orientations used. (The parameters A and D contain all of the interesting physics of the model; the other parameters used in the computer program described previously exist solely for the purpose of orienting the ligand nuclei and magnetic field relative to the g-tensor axis system.)

Also, values of D_j scaled as $(1/r_j)^3$ were tried in order to test the hypothesis that the interaction can be described as that between classical point dipoles alone. Though these values could be scaled overall to give reasonable results, the fits were judged to be not as good as for those curves with all the D_j equal.

The value of D controlled the depth of the modulation as well as the modulation frequency. This parameter was fit first because the model behaves more predictably for variations in D, and because the model is more sensitive to D. The parameter

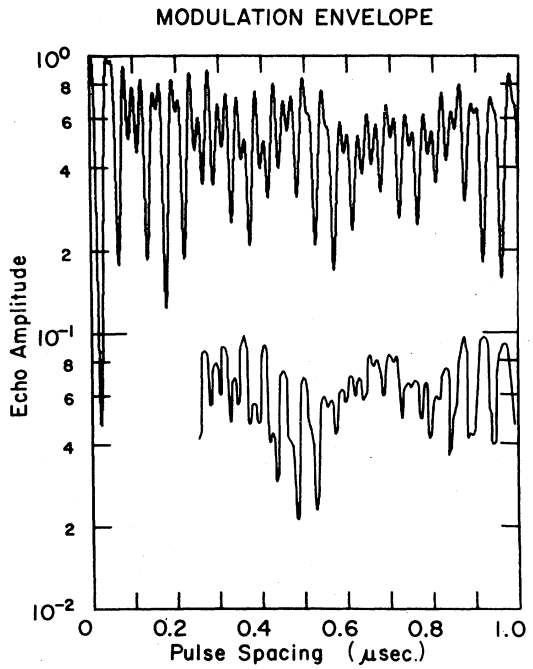

FIG. 5. Upper curve is the calculated echo envelope from the computer program for A_{lab} equal to 144° (see Table I). The applied field is +10° from the y axis of the g tensor in a plane approximately perpendicular to the c axis of the crystal. The lower curve is the measured echo envelope with the relaxation decay removed. Echo amplitude is in arbitrary units and the pulse spacing is the time, in microseconds, between the two microwave pulses.

A tended to change the locations of the large amplitude points on the curves, in a very complex fashion.

After D had been varied in 1-MHz increments over the range 3–6 MHz with A set equal to 0, the best values of D were then used while different values of A were tried in the model. The values of D which gave the best fits were $D=4$ and 5 MHz. Letting A assume values in the range (–) 3–2 MHz led to the conclusion that A lies near −1.5 MHz. The constraint that the same or nearly the same value of A must fit for all orientations of H_0 yielded the value of A quoted; otherwise, at a given orientation several good values of A could be found and the proper choice would not be obvious. At those orientations where the g value is the largest at which data was taken, the determinations of A were most obvious. The position of minimum g value gave theoretical results that were relatively insensitive to variations in A. The results of the comparison of the theoretical model to the experimental data yield $D=4\pm1$ MHz, $A=-1.5\pm0.5$ MHz.

The value of D which is quoted above is lower than the value of D used in the theoretical plots displayed for the following reason: The method of signal detection is nonlinear. Studies on the system have shown that the voltages displayed on the oscilloscope for the modulation envelopes studied are approximately proportional to the power present in the echo signal. This means that the modulation envelopes calculated from the theoretical model should be squared before being plotted for comparison to the experimental data. When a given modulation envelope is squared the depth of modulation is doubled, so that smaller values of D are needed to give equivalent depths of modulation. Some experimentation with the model showed that the linear case yielded D between 4 and 5 MHz and that the "squared" case yielded D between 3 and 4 MHz. In the final analysis, it was the general character of the modulation curves which were compared; the depth was only one of several features considered. Good fits could be obtained for the "squared" case with $D=4$ MHz and $A=-1.5\pm0.5$ MHz. The plots shown are for the linear case.

There is no doubt that the negative values of A give better results than the positive values. At the peak of the resonance line the fits improve greatly for the negative values of A.

Lastly, it is interesting to note that the computer model showed that at the crossing point of the two resonance lines which peak at different angles; the theoretical modulation curves are identical for both lines. This shows that at this orientation H_0 has equivalent directions relative to the ligand group, even though the orientations are not the same.

Without a complete theoretical analysis of the wave functions for the $4f$ electrons of Nd^{3+} substituted in LaF_3, definite conclusions are difficult if not impossible to make. Although accurate wave functions are available for the free Nd^{3+} ion,[31-34] they are expressed in a form which makes a simple physical interpretation impossible; it is not correct to think of the electronic wave functions as consisting of symmetrically located lobes protrud-

TABLE I. Summary of experimental results: Best choices of model parameters at different orientations.

A_{lab}	A (MHz)	D (MHz)
124°	−1.5	5
129°	−2	5
134°	−1	5
139°	−1	5
144°	−1.5	5

TABLE II. Comparison of endor results for $CaF_2:R^{3+}$ with $LaF_3:Nd^{3+}$.

		A_S/g (MHz)	A_P/g (MHz)	A_D/g (MHz)	g	Reference
$4f^7$	$CaF:Eu^{2+}$	−1.11	2.0	2.25	2.00	40
$4f^7$	$CaF_2:Gd^{3+}$	−0.925	2.53	2.81	1.99	41
$4f^{13}$	$CaF_2:Tm^{2+}$	0.75	3.56	2.84	3.45	38 and 42
$4f^{13}$	$CaF_2:Yb^{3+}$	0.49	5.12	2.85	3.44	43
$4f^3$	$LaF_3:Nd^{3+}$	−1.5	4	1.7–2.6	1.0	This work

ing from the Nd nucleus; in the case of $4f$ electrons the angular momentum is unquenched and hence the lobes normally associated with electronic orbitals are now rotating. Furthermore the linear combinations of $|JM_j\rangle$ states are sufficiently complex that conceptualizing a physical interpretation is impossible in a case of such low symmetry as LaF_3. Unlike the situation for d electrons, the case for f electrons does not lend itself to simple pictures.

Computations of $4f$ wave functions have been carried out in several cases; the most complete seem to be those of Freeman and Watson.[31,35,36] These authors have shown that unrestricted Hartree-Fock calculations lead to interesting but difficult interpretations of the hyperfine interactions of $4f$ electrons. Direct $4f$-ligand and covalency produce spin densities at the ligand sites with the same sign as that in the $4f$ shell. However, core polarization with covalency and overlap of $5s$ or $5p$ orbitals or empty $6s$ orbitals produce spin densities at the ligand sites with the opposite sign as that in the $4f$ shell. This is discussed by McGarvey[37] and by Watson.[39]

The best comparison which can be made for the results of this work is the comparison with the numbers found from ENDOR studies of other rare-earth-ion fluoride complexes. These are summarized in Tables I and II. As can be seen from Tables I and II the results of this experiment are in reasonable agreement with those for other rare-earth ions in CaF_2, as far as magnitudes go. The signs of the isotropic parameter present a puzzle. As far as can be learned, no ENDOR measurements have been made on defect free sites in the system $CaF_2:Nd^{3+}$. Bear in mind when using Tables I and II that the lattice distances in LaF_3 are larger than the nearest-neighbor spacing in CaF_2, and that they are unequal among the ligand sites.

*Present address: Scientific-Atlanta, Inc., Atlanta, Georgia.

[1]L. G. Rowan, E. L. Hahn, and W. B. Mims, Phys. Rev. A 137, 61 (1965).

[2]W. B. Mims, K. Nassau, and J. D. McGee, Phys. Rev. 123, 2059 (1961).

[3]J. A. Cowen and D. E. Kaplan, Phys. Rev. 124, 1098 (1961).

[4]F. C. Newman and L. G. Rowan, Phys. Rev. B 5, 4231 (1972).

[5]W. B. Mims, Phys. Rev. B 5, 2409 (1972).

[6]W. B. Mims, Phys. Rev. B 6, 3543 (1972).

[7]W. B. Mims, in *Electron Paramagnetic Resonance*, edited by S. Geschwind (Plenum, New York, 1972), Chap. 4.

[8]P. F. Liao and S. R. Hartman, Phys. Rev. B 8, 69 (1973).

[9]D. Grischkowsky and S. R. Hartman, Phys. Rev. B 2, 60 (1970).

[10]L. Q. Lambert, Phys. Rev. B 7, 1834 (1973).

[11]A. Abragam and B. Bleaney, *Electron Paramagnetic Resonance of Transition Ions* (Oxford University, Oxford, 1970).

[12]G. Feher, Phys. Rev. 103, 834 (1956).

[13]G.H. Dieke, *Spectra and Energy Levels of Rare Earths* (Wiley, New York, 1968).

[14]W. F. Krupke, Phys. Rev. 145, 325 (1966).

[15]S. A. Johnson, H. G. Freie, and A. L. Schawlow, J. Opt. Soc. Am. 57, 734 (1967).

[16]R. P. Bauman and S. P. S. Porto, Phys. Rev. 161, 842 (1967).

[17]V. K. Sharma, J. Chem. Phys. 54, 496 (1971).

[18]I. Oftedal, Z. Phys. Chem. B 13, 190 (1931).

[19]K. Schlyter, Arkiv. Kemi. 5, 73 (1953).

[20]M. Mansmann, Z. Kristallogr. 122, 375 (1965).

[21]A. Zalkin, D. H. Templeton, and T. E. Hopkins, Inorg. Chem. 5, 1466 (1966).

[22]H. E. Rast, H. H. Caspers, S. A. Miller, and R. A. Buchanan, Phys. Rev. 171, 1051 (1968).

[23]R. P. Lowndes, J. F. Parrish, and C. H. Perry, Phys. Rev. 182, 913 (1969).

[24]J. M. Baker, R. S. Rubins, Proc. Phys. Soc. Lond. 78, 1353 (1961).

[25]M. B. Schulz and C. D. Jeffries, Phys. Rev. 149, 270

(1966).
[26]E. Y. Wong, O. M. Staffsudd, and D. R. Johnston, Phys. Rev. 131, 990 (1963).
[27]L. O. Anderson and G. Johansson, Z. Kristallogr. 127, 386 (1968).
[28]R. J. Rachford and C. Y. Huang, Phys. Rev. B 3, 2121 (1971).
[29]J. M. Baker, W. Hays, and M. C. M. O'Brien, Proc. R. Soc. A 254, 273 (1960).
[30]See Ref. 7, p. 311 (footnote).
[31]A. J. Freeman and R. E. Watson, Phys. Rev. 127, 2058 (1962).
[32]M. Synek and L. Corsiglia, J. Chem. Phys. 48, 3121 (1968).
[33]M. Sunek and P. Grossgut, Phys. Rev. A 1, 1 (1970).
[34]B. G. Wybourne, J. Chem. Phys. 34, 279 (1961).
[35]A. J. Freeman and R. B. Frankel, *Hyperfine Interactions* (Academic, New York, 1967), Chap. 2.
[36]R. E. Watson and A. J. Freeman, Phys. Rev. Lett. 6, 277 (1961).
[37]B. R. McGarvey, J. Chem. Phys. 65, 955 (1976).
[38]J. M. Baker and W. B. J. Blake, Phys. Lett. A 31, 61 (1970).
[39]R. E. Watson, P. Bagus, and A. J. Freeman, Bull. Am. Phys. Soc. 13, 482 (GH6) (1968).
[40]J. M. Baker and J. P. Hurrell, Proc. Phys. Soc. 82, 742 (1963).
[41]H. Bill, Phys. Lett. A 29, 593 (1969).
[42]R. G. Bessent and W. Hays, Proc. R. Soc. A 285, 430 (1965).
[43]U. Ranon and J. S. Hyde, Phys. Rev. 141, 259 (1966).